Quantum-size effects in thin metallic films

Alexey Yu. Aladyshkin

Moscow Institute for Physics and Technology, Dolgoprudny

Institute for Physics of Microstructures Russian Academy of Sciences, Nizhny Novgorod

Lobachevsky State University of Nizhny Novgorod, Nizhny Novgorod

National Research University Higher School of Economics, Moscow

E-mail: aladyshkin.au@mipt.ru, aladyshkin@ipmras.ru

Russian-Chinese International School
"Superconducting functional materials for advanced quantum technologies"
25^{th} – 29^{th} September 2023, Dolgoprudny

Outline

* **Introduction**
    - Scattering problem: quantum-well states and resonant tunneling
    - Scanning tunneling microscopy and spectroscopy
* **Quantum-well states for electrons *in* Pb(111) films**
    - Tunneling interferometry and commensurability effect
    - Estimates of microscopic parameters
    - Visualization of hidden defects
    - Oscillations of visible height of monatomic steps
* **Quantum-well states for electrons *above* Pb(111) films**
    - Image-potential states and Stark-shifted image potential states
    - Gundlach oscillations and field-emission resonances
    - Estimate of local work function
    - Periodic variations of $d(\ln I)/dz$ as a function of STM-tip height
    - Estimate of absolute height of a STM-tip height above a sample surface
* **Summary and list of main publications**

Introduction

Quantum particle in a box: quantum-well states

Let us consider one-dimensional potential well $U(z)$ of arbitrary shape.

Let us assume that there is a region with constant potential energy inside the well. We introduce two reflection amplitudes r_1 and r_2', which characterize the reflection of electronic waves from the left and right edges, respectively.

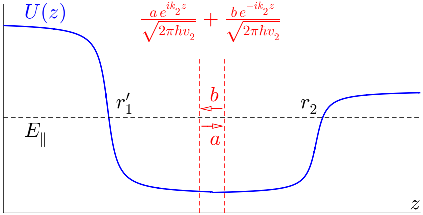

Reflections of electrons at the left and right barriers are described by relationships $a = r_1' b$ and $b = r_2 a$, therefore

$$a = r_1' b = r_1' r_2\, a \qquad \Longrightarrow \qquad (1 - r_1' r_2)\, a = 0.$$

Nontrivial solutions ($a \neq 0$ and $b \neq 0$) exist under the condition

$$1 - r_1' r_2 = 0.$$

Since $r_1' = 1 \cdot e^{i \arg r_1'}$ and $r_2 = 1 \cdot e^{i \arg r_2}$, then the condition $r_1'\, r_2 = 1$ can be rewritten in the form

$$1 \cdot e^{i \arg r_1' + i \arg r_2'} = 1 \cdot e^{i\, 2\pi n} \qquad \Longrightarrow \qquad \arg r_1' + \arg r_2 = 2\pi n, \quad n = 0, 1, \ldots$$

Coherent resonant tunneling in a double-barrier structure

Assume that the the potential $U(z)$ can be considered as a combination of two localized scatters (barriers or steps) $U_1(z)$ and $U_2(z)$. How to calculate the resulting coefficient of transmission?

We apply a perturbation theory, formally assuming that all reflection coefficients are rather small:

zero-order term: $t^{(0)} = t_2\, t_1$

first-order term: $t^{(1)} = t_2\, r_1'\, r_2\, t_1$

$n-$th order term: $t^{(n)} = t_2\, (r_1'\, r_2)^n\, t_1$

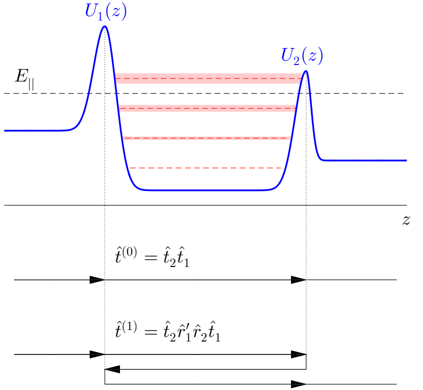

Transmission amplitude
$$t = \sum_{n=0}^{\infty} t^{(n)} = \sum_{n=0}^{\infty} t_2\, (r_1' r_2)^n\, t_1 = \frac{t_2\, t_1}{(1 - r_1' r_2)} \quad \text{if} \quad 1 - r_1' r_2 \neq 0$$

Transmission coefficient
$$\mathcal{T} = \left| \frac{t_1 t_2}{1 - r_1' r_2} \right|^2 = \frac{\mathcal{T}_1\, \mathcal{T}_2}{1 + \mathcal{R}_1 \mathcal{R}_2 - 2\sqrt{\mathcal{R}_1 \mathcal{R}_2} \cos\left(\arg r_1' + \arg r_2\right)}.$$

The conditions $1 - r_1' r_2 = 0$ and $arg\ r_1' + arg\ r_2 = 2\pi n$ correspond to the localized stationary or quasi-stationary electronic states in a one-dimensional quantum well.

Scanning tunneling microscopy (STM): general scheme

Invention: Binnig & Rohrer (1981), Nobel prize in physics (1986)

This approach is applicable only for conducting samples

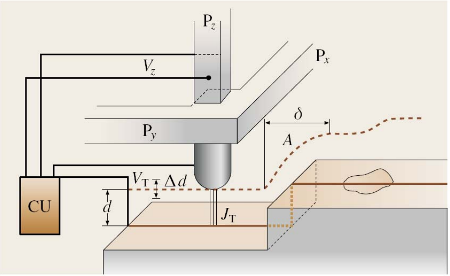

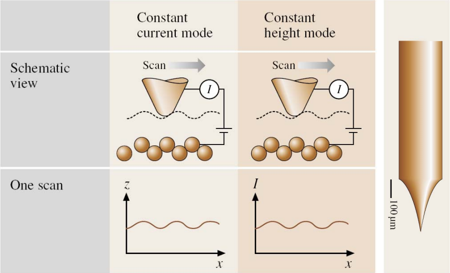

Binnig, Rohrer, Gerber, ... Phys. Rev. Lett., vol. 49, 57–61 (1982)

Binnig and Rohrer, Surf. Sci. vol. 126, 236–244 (1983)

Chen, *Introduction to scanning tunneling microscopy.* Oxford (1993)

Wiesendanger, *Introduction to scanning probe ...* Cambridge (1994)

Springer Handbook of Nanotechnology (Ed. B. Bhushan), part C (2010)

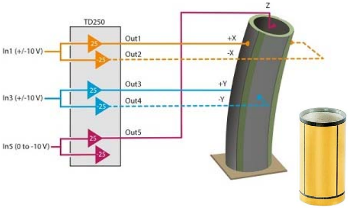

Single-point tunneling spectroscopy

Measurement of local current-voltage ($I - V$) dependence at a fixed position of the STM tip with respect to the sample surface

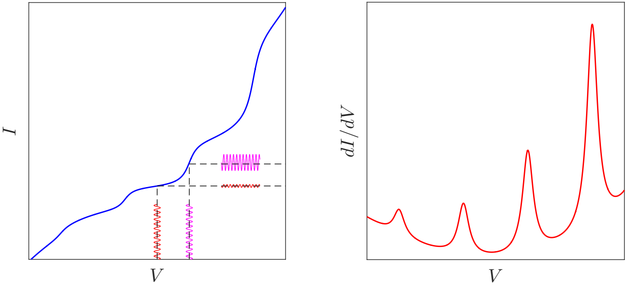

Modulation technique: $V(t) = V_0 + V_1 \cdot cos\,\omega t \quad \Longrightarrow \quad I(t) = I_0 + I_1 \cdot cos\,(\omega t + \gamma)$

$$I_1 \simeq V_1 \cdot \left(\frac{dI}{dV}\right)_{V_0}$$

Thus, the amplitude of the oscillation of tunneling current measured by a lock-in amplifier is proportional to the differential tunneling conductance dI/dV at given mean bias voltage $V = V_0$.

Scanning grid spectroscopy

During scanning process the STM tip periodically stops for the acquiring the local $I - V$ dependences at fixed positions of the STM tip with respect to the sample surface.

Results of measurements: three arrays $z = f(x_n, y_m, V_0)$, $I = f(V, x_n, y_m)$ and $dI/dV = f(V, x_n, y_m)$.

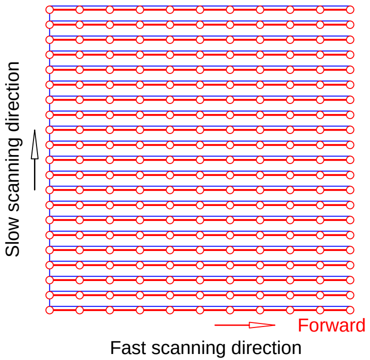

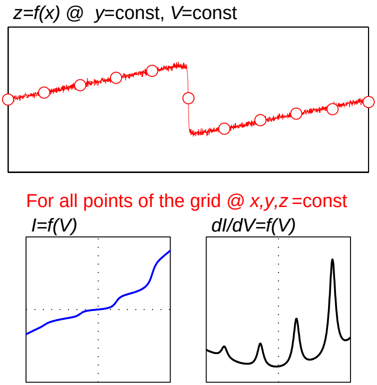

Scanning tunneling microscopy/spectroscopy in a modulation regime

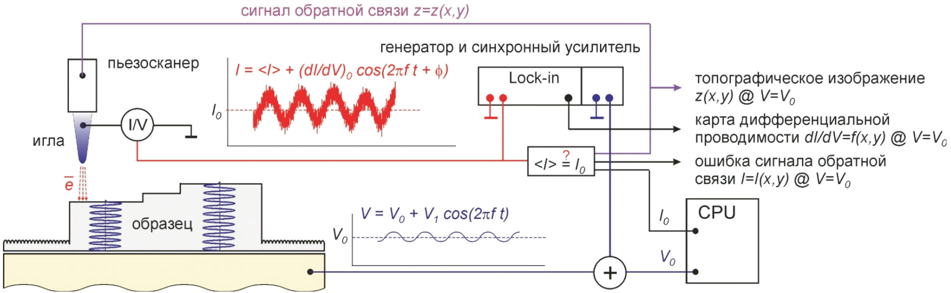

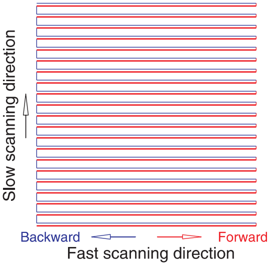

$z=f(x)$ @ y=const, V=const

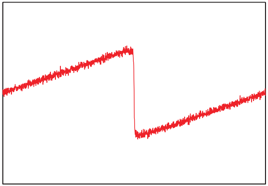

$dI/dV=f(x)$ @ y=const, V=const

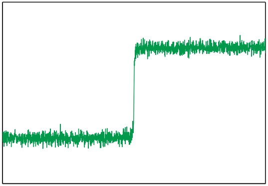

Quantum-well states
for electrons in Pb(111) films

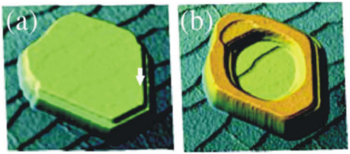

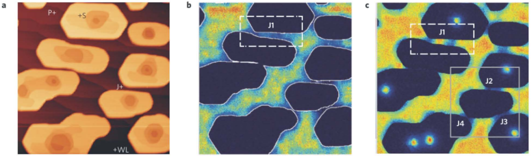

Figures are taken the following papers

Li *et al.* Appl. Phys. Lett., vol. 89, 123111 (2006)

Roditchev *et al.* Nature Physics, vol. 11, 332 (2015)

References: properties of thin and ultrathin Pb films (1)

Growth mechanisms

Zhang *et al. Electronic growth of metallic overlayers ...* Phys. Rev. Lett. 80, 5381 (1998)

Materzanini *et al. Quantum size effects in metal films ...* Phys. Rev. B 63, 235405 (2001)

Wei and Chou, *Theory of quantum size effects in thin Pb(111) films.* Phys. Rev. B 66, 233408 (2002)

Fokin *et al. Electronic growth of Pb on the vicinal Si surface.* Phys. Stat. Solidi (c) 7, 165 (2010)

Transport properties

Jalochowski *et al. Experimental evidence for quantum-size-effect ...* Phys. Rev. B 45, 13607 (1992)

Jalochowski *et al. Quantized Hall effect in ultrathin metallic films ...* Phys. Rev B 76, 4227 (1996)

Miyata *et al. Electronic transport properties of quantum-well states ...* Phys. Rev B 78, 245405 (2008)

Electronic properties and tunneling spectroscopy

Jaklevic *et al. Observation of electron standing waves in a crystalline box.* Phys. Rev. Lett. 26, 88 (1971)

Jaklevic *et al. Experimental study of quantum size effects in thin metal ...* Phys. Rev. B 12, 4146 (1975)

Altfeder *et al. Electron fringes on a quantum wedge.* Phys. Rev. Lett. 78, 2815 (1997)

Altfeder *et al. Imaging buried interfacial lattices with quantized electrons.* Phys. Rev. Lett. 80, 4895 (1998)

Su *et al. Correlation between quantized electronic states and oscillatory ...* Phys. Rev. Lett. 86, 5116 (2001)

Altfeder *et al. Imaging subsurface reflection phase with quantized ...* Phys. Rev. Lett. 88, 206801 (2002)

Eom *et al. Persistent superconductivity in ultrathin Pb films ...* Phys. Rev. Lett. 96, 027005 (2006)

Hong *et al. Decay mechanisms of excited electrons in quantum-well ...* Phys. Rev. B 80, 081409 (2009)

Hsu *et al. Effects of electronic confinement and substrate on the low ...* Surf. Sci. 604, 1 (2010)

Kim *et al. Influence of quantum well states ... ultra-thin Pb films.* Surf. Sci. 632, 174 (2015)

References: properties of thin and ultrathin Pb films (2)

Electronic properties and photoemission spectroscopy

Mans *et al. Quantum electronic stability and spectroscopy of ultrathin ...* . Phys. Rev. B 66, 195410 (2002)

Milun *et al. Quantum oscillations in Pb/Si (111) heterostructure system*. Rep. Prog. Phys. 65, 99 (2002)

Upton *et al. Unusual band dispersion in Pb films on Si(111)*. Phys. Rev. B 71, 033403 (2005)

Dil *et al. Electron localization in metallic quantum wells ...* Phys. Rev. B 73, 161308 (2006)

Dil *et al. Rashba-type spin-orbit splitting of quantum well states in ...* Phys. Rev. Lett. 101, 266802 (2008)

Ricci *et al. Analyticity of the phase shift and reflectivity of electrons ...* Phys. Rev. B 79, 195433 (2009)

Dil *et al. Influence of the substrate lattice structure on ...* J. Phys.: Condens. Matter. 22, 135008 (2010)

Superconducting properties

Cren *et al. Ultimate vortex confinement studied by scanning ...* Phys. Rev. Lett. 102, 127005 (2009)

Cren *et al. Vortex fusion and giant vortex states ...* Phys. Rev. Lett. 107, 097202 (2011)

Nishio *et al. Superconductivity of nanometer-size Pb islands ...* Appl. Phys. Lett. 88, 113115 (2006)

Nishio *et al. Superconducting Pb island nanostructures studied ...* Phys. Rev. Lett. 101, 167001 (2008)

Qin *et al. Superconductivity at the two–dimensional limit.* Science 324, 1314 (2009)

Ning *et al. Vortex properties of two-dimensional Pb films.* J. Phys.: Condens. Matt. 22, 065701 (2010)

Zhang *et al. Superconductivity in one-atomic-layer metal films ...* Nature Physics 6, 104 (2010)

Cherkez *et al. Proximity effect between two superconductors ...* Phys. Rev. X 4, 011033 (2014)

Werner *et al. Domain-wall and reverse-domain superconducting ...* Phys. Rev. B 84, 020505(R) (2011)

Moore *et al. Low-temperature scanning tunneling microscopy ...* Supercond. Sci. Technol. 28, 045003 (2015)

Roditchev *et al. Direct observation of Josephson vortex cores.* Nature Physics 11, 332 (2015)

Standing electronic waves in Pb(111) films

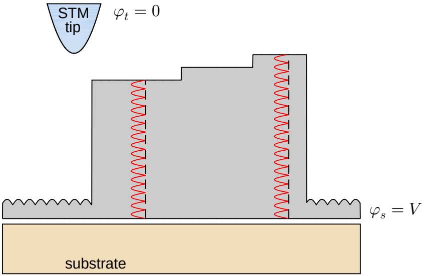

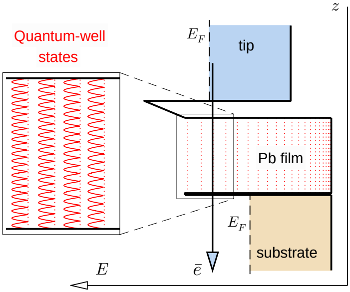

Set of allowed values of wave vector $k_n = \pi n/D$, where $D = N\, d_{ML}$ is the actual thickness of the film, $d_{ML} = 0.286$ nm is the height of the Pb(111) monolayer.

Set of the energy E_n for quantum-well states

$$E_n^{(N)} \simeq E_0 + \frac{\hbar^2 k_n^2}{2m^*} \simeq E_0 + \frac{\hbar^2}{2m^*}\left(\frac{\pi\, n}{D}\right)^2 \simeq E_F + \hbar v_F \cdot \left(\frac{\pi n}{N\, d_{ML}} - \frac{2\pi}{\lambda_F}\right) \quad \text{at} \quad k \simeq k_F.$$

Provided that $\lambda_F : d_{ML} = 4 : 3$ and $N \gg 1$, we get $E_n^{(N)} \simeq E_{n+3}^{(N+2)}$.

Tunneling interferometry: typical experimental results

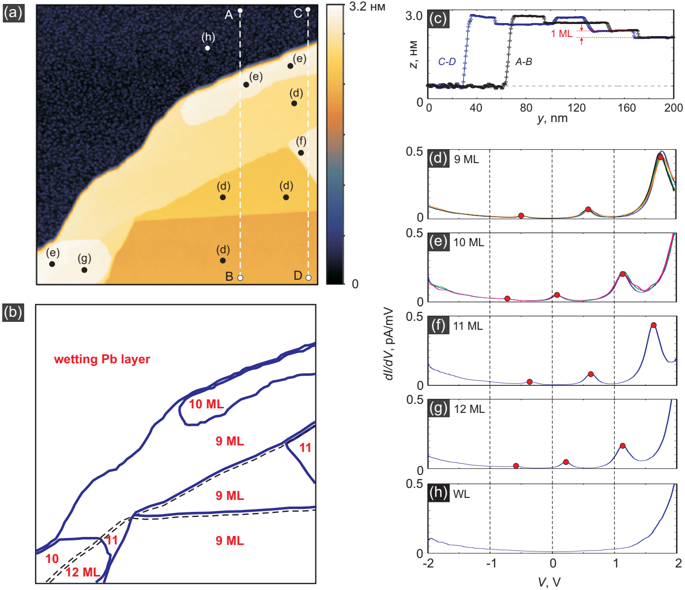

$115 \times 115\ \mathrm{nm}^2$, $V_0 = +2000\ \mathrm{mV}$, $I = 50\ \mathrm{pA}$

Quantum-well states for thin Pb(111) films

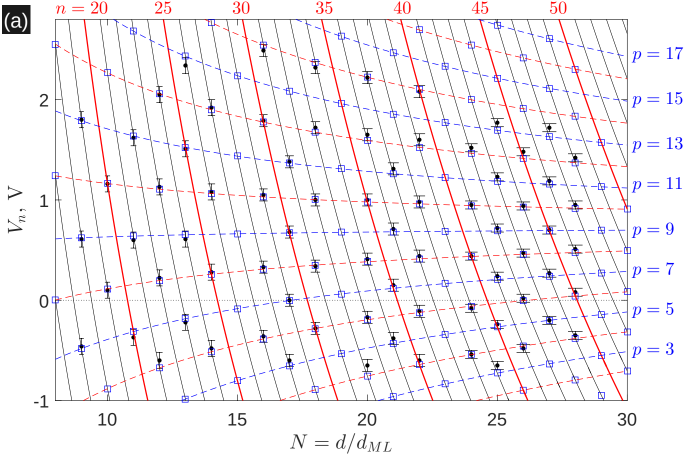

lines of constant n: $$E_n \simeq E_F + \hbar v_F \cdot \left(\frac{\pi n}{d_{WL} + N\, d_{ML}} - k_F \right)$$

line of constant $p = 2n - 3N$: $$E_p \simeq E_F + \hbar v_F \cdot \left(\frac{3\pi}{2 d_{ML}} \cdot \frac{(N + p/3)}{(N + d_{WL}/d_{ML})} - k_F \right)$$

Determination of microscopic parameters of Pb(111) films

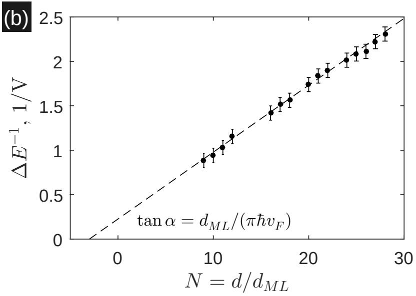

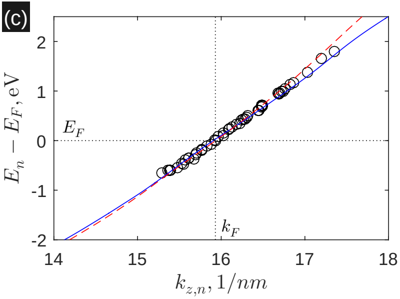

$$E_n \simeq E_F + \hbar v_F \cdot \left(\frac{\pi n}{d_{WL} + N\, d_{ML}} - k_F \right) \quad \Longrightarrow \quad \Delta E = E_{n+1} - E_n = \frac{\pi \hbar v_F}{(d_{WL} + N\, d_{ML})}$$

Thickness of wetting layer:	$d_{WL} \simeq 3\, d_{ML}$
Fermi velocity:	$v_F \simeq 1.84 \cdot 10^8$ cm/s
Fermi wave vector:	$k_F \simeq 15.94\, \mathrm{nm}^{-1}$
Fermi wave length:	$\lambda_F \simeq 0.394$ nm
Effective mass:	$m^* \simeq 1.01\, m_0$

Visualization of terraces of different actual height

Parallel acquisition of the topography map $z = z(x, y)$ and the map of differential tunneling conductance $dI/dV = f(x, y)$ allows to visualize hidden structural defects like monatomic steps in substrate, foreign inclusions, areas with mechanical stress and non-quantized variations of the height

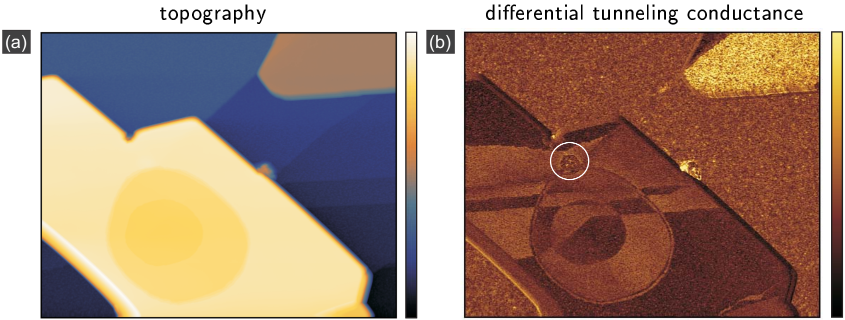

$450 \times 350\,\mathrm{nm}^2$, $V_0 = +300\,\mathrm{mV}$, $I = 200\,\mathrm{pA}$

Visualization of subsurface dislocation lines (1)

topography | current map | differential tunneling conductance

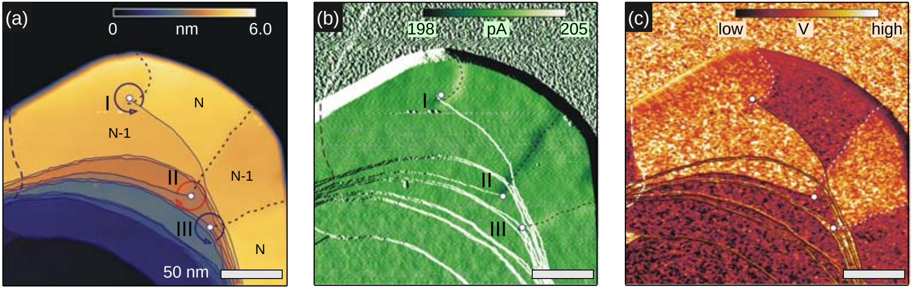

$232 \times 232\,\mathrm{nm}^2$, $V_0 = 700\,\mathrm{mV}$, $I = 400\,\mathrm{pA}$

Fermi energy of electronic gas

$E_F = (\hbar^2/2m^*) \cdot (3\pi^2 n_{el})^{2/3}$

Jump of electronic density

$\delta n_{el} \sim n_{el}/N$

Shift of Fermi energy

$\delta E_F \sim 2E_F^{(0)}/(3N)$

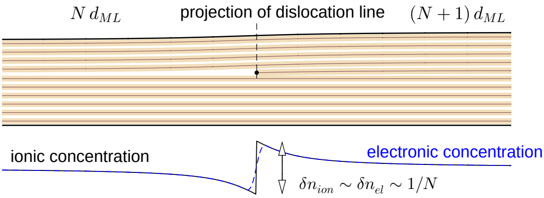

Visualization of subsurface dislocation lines (2)

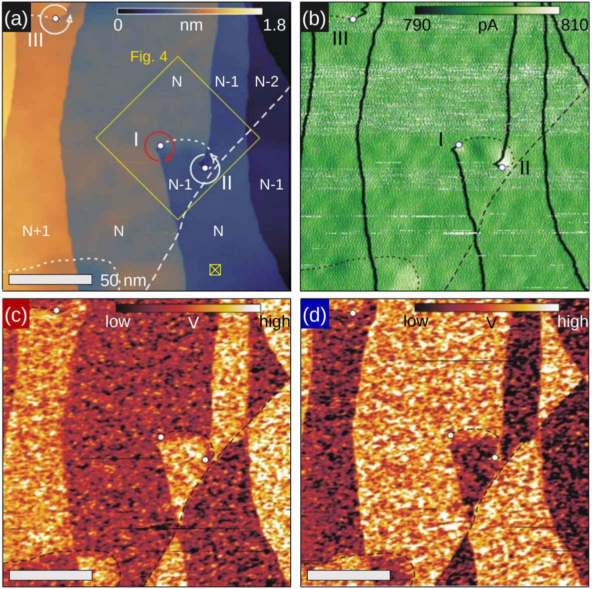

$174 \times 174\ \mathrm{nm}^2$, $V_0 = 700$ and 900 mV, $I = 800$ pA

Terraces with non-quantized height variations (1)

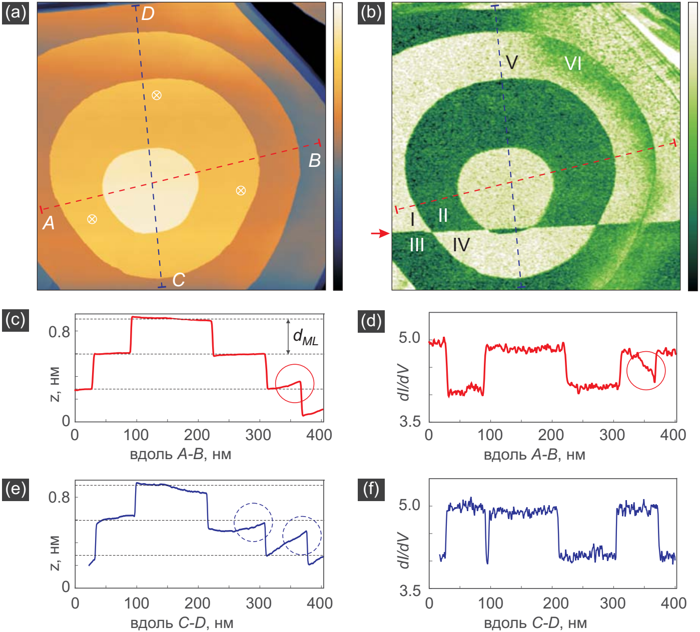

Terraces with non-quantized height variations (2)

$1160 \times 1160\,\mathrm{nm}^2$, $V_0 = 600$ and $900\,\mathrm{mV}$, $I = 200\,\mathrm{pA}$

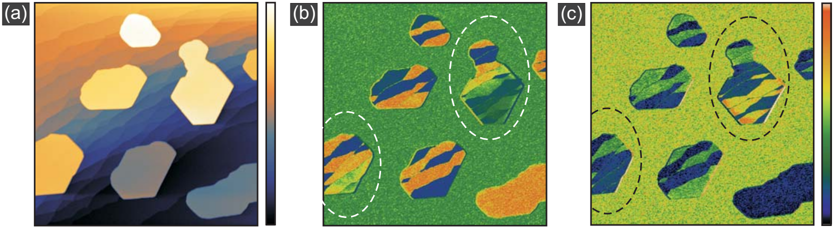

$230 \times 230\,\mathrm{nm}^2$, $V_0 = 900$ and $950\,\mathrm{mV}$, $I = 600\,\mathrm{pA}$

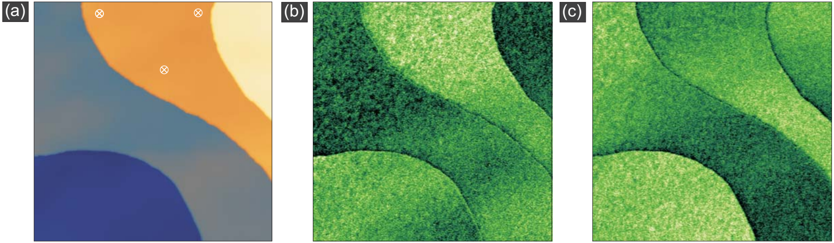

Oscillations of visible height of the monatomic Pb(111) step

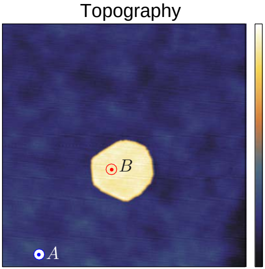

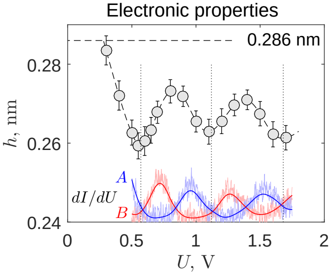

point A – 23 monolayers, point B – 24 monolayers

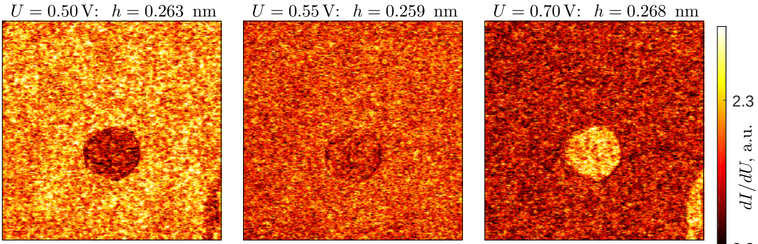

intermediate height | minimal height | intermediate height

Quantum-well states for electrons above Pb(111) films

Photos of lenticular clouds are taken from Internet

References: image-potential states (1)

Echenique and Pendry, J. Phys. C: Solid State Phys. 11, 2065 (1978)

McRae, *Electronic surface resonances of crystals.* Rev. Mod. Phys. 51, 541 (1979)

Smith, *Phase analysis of image states and surface states ...* Phys. Rev. B 32, 3549 (1985)

Garcia *et al. Image states: Binding energies ...* Phys. Rev. Lett. 54, 591 (1985)

Echenique and Pendry, *Theory of image states at metal surfaces.* Prog. Surf. Sci. 82, 111 (1990)

Chulkov *et al. Image potential states on metal surfaces ...* Surf. Sci. 437, 330 (1999)

Gundlach, *Zur berechnung des tunnelstroms durch eine trapezformige ...* Solid-State Electr. 9, 949 (1966)

Kolesnychenko *et al. Field-emission resonance measurements ...* Physica B 291, 246 (2000)

Kolesnychenko *et al. Calibration of the distance ...* Rev. Sci. Instr. 70, 1442 (1999)

Garcia *et al. Distance–voltage characteristics ...* J. Phys. C: Solid State Phys. 19, L131 (1986).

Becker *et al. Electron interferometry at crystal surfaces.* Phys. Rev. Lett. 55, 987 (1985)

Binnig *et al. Tunneling spectroscopy and inverse photoemission ...* Phys. Rev. Lett. 55, 991 (1985)

Wahl *et al. Quantum coherence of image-potential states.* Phys. Rev. Lett. 91, 106802 (2003)

Hanuschkin *et al. Image potential and field states ...* Phys. Rev. B 76, 165417 (2007)

Kubetzka *et al. Spin–polarized scanning tunneling microscopy ...* Appl. Phys. Lett. 91, 012508 (2007)

Silkin *et al. Image potential states in graphene.* Phys. Rev. B 80, 121408(R) (2009)

Ge *et al. Probing image potential states on the surface ...* Phys. Rev. B 101, 035152 (2020)

Jung *et al. Identification of metals in scanning tunneling ...* Phys. Rev. Lett. 74, 1641 (1995)

Rienks *et al. Surface potential of a polar oxide film ...* Phys. Rev. B 71, 241404(R) (2005)

References: image-potential states (2)

Pivetta *et al. Local work function Moire pattern on ultrathin ...* Phys. Rev. B 72, 115404 (2005)

Ploigt *et al. Local work function changes determined ...* Phys. Rev. B 76, 195404 (2007)

Lin *et al. Manifestation of work function difference ...* Phys. Rev. Lett. 99, 216103 (2007)

Borisov *et al. Image potential states of supported metallic ...* Phys. Rev. B 76, 121402(R) (2007)

Yang *et al. Phase contribution of image potential on empty ...* Phys. Rev. Lett. 102, 196102 (2009)

Becker *et al. Scattering and lifetime broadening ...* Phys. Rev. B 81, 205438 (2010)

Zugarramurdi *et al. Theoretical study of constant current ...* Phys. Rev. B 84, 115422 (2011)

Schouteden *et al. Quantum confinement of hot image–potential...* Phys. Rev. Lett. 103, 266805 (2009)

Schouteden *et al. Lateral quantization of two–dimensional ...* Phys. Rev. Lett. 108, 076806 (2012)

Schouteden *et al. Probing quantized image–potential states ...* Nanotechnology 21, 485401 (2010)

Stepanow *et al. Localization, splitting, and mixing ...* Phys. Rev. B 83, 115101 . (2011)

Craes *et al. Mapping image potential states on graphene quantum dots.* Phys. Rev. Lett. 111, 056804 (2013)

Yamada *et al. Spectroscopic investigation of unoccupied states...* J. Phys. Chem. C. 118, 1035 (2014)

Sugawara *et al. Interaction of Stark–shifted image potential states...* Phys. Rev. B 96, 075444 (2017)

Bono *et al. Conductance oscillations in scanning tunneling ...* Surf. Sci. 188, 153 (1987)

Image potential in electrostatics

It is known that a probe charge located outside a conductive sample generate a charge at the surface of the opposite sign. The interaction of the probe charge with the charged flat surface of bulk sample can be viewed as the electrostatic interaction of the probe charge and the mirror (image) charge. A Coulomb force acting between point charges e and $-e$ at a distance $2h$ as well as corresponding potential are equal

$$F_z(h) = -\frac{1}{\varepsilon}\,\frac{e^2}{(2h)^2} \quad \text{and} \quad U(z) = E_{vac} - \int\limits_z^{+\infty} F_z(h')\,dh' = E_{vac} - \frac{1}{\varepsilon}\,\frac{e^2}{4z}.$$

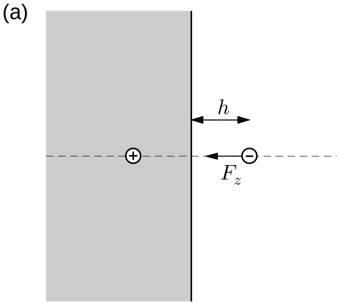

The image potential resembles the Coulomb potential for hydrogen atom in one dimension

Surface electronic states in the image potential (1)

If the energy of the image-potential states is in the forbidden band of bulk crystal, such localized electronic states can be quasi-stationary and slowly decaying, affecting optical and transport properties of nanostructured samples.

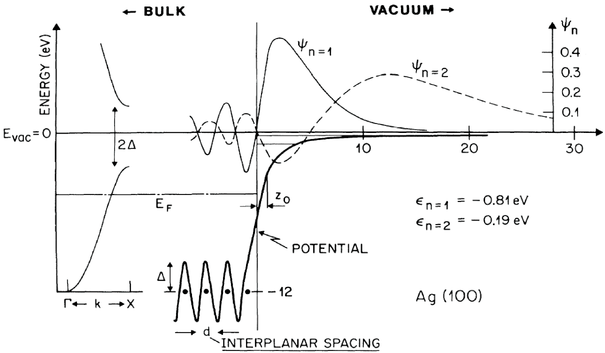

FIG. 2. Energy and spatial scales characterizing image states on metal surfaces. Shown are the fundamental ($n=1$) image state, with no nodes in the vacuum region, and the first excited ($n=2$) image state, with one node. Also shown are the effective one-electron potential and the bulk energy-band structure that produce these image states. The quantity z_0 (taken to be ~1 Å) specifies the distance from the surface beyond which the potential is purely Coulombic (imagelike). The parameters Δ, width of the gap, its position, and the Fermi energy E_F have been taken from self-consistent band-structure calculations (Ref. 12). The image plane corresponds to $z=0$.

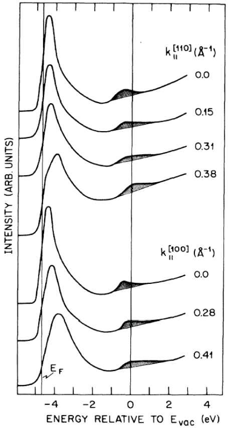

Garcia, Reihl, Frank, and Williams, Phys. Rev. Lett., vol. 55, 991-994 (1985)

Surface electronic states in the image potential (2)

Let us assume that (i) $E_{vac} = 0$ and (ii) the energy of the localized states belongs to the forbidden band of bulk crystal. The effective potential for non-transparent wall at $z = 0$ can be written in the form

$$U(z) = \begin{cases} \infty & \text{at } z < 0, \\ -e^2/4z & \text{at } z > 0, \end{cases}$$

where z is the distance measured from the surface, $a = 0$ and $b = e^2/4|E_n|$ are classical turning points for a particle with energy $E_n = -|E_n|$.

Within quasi-classical Wentzel-Kramers-Brillouin (WKB) approximation, one can estimate the change of the phase of the electronic wave function for the round trip ($a \to b \to a$)

$$\frac{1}{\hbar} \int_a^b p(z)\, dz + \varphi_b + \frac{1}{\hbar} \int_b^a (-p(z))\, dz + \varphi_a = 2\pi n,$$

where φ_a and φ_b are the phase shifts for reflected waves at points a and b, correspondingly; $n = 0, 1 \ldots$ is the number of quantum-well state.

After rearranging, we come to the Bohr-Sommerfeld quantization rule

$$\frac{1}{2\pi\hbar} \oint p(z)\, dz = n + \gamma, \quad \text{where} \quad \gamma = -\frac{\varphi_a}{2\pi} - \frac{\varphi_b}{2\pi} \simeq \frac{3}{4}.$$

Surface electronic states in the image potential (3)

Afetr substituting $p(z) = \sqrt{2m_0 \left(E - U(z)\right)}$ into the Bohr-Sommerfeld quantization rule, we get

$$\frac{1}{2\pi\hbar} \oint p(z)\, dz = \frac{1}{\pi\hbar} \int\limits_0^b \sqrt{2m_0 \left(E_n - U(z)\right)}\, dz = \frac{e^2}{\pi\hbar} \sqrt{\frac{2m_0}{|E_n|}}\, \frac{\pi}{8} = n + \gamma.$$

As a result, the spectrum of the localized electronic states in the image-potential with non-penetrable well is given by a simple relationship

$$E_n = -\frac{m_0 e^4}{32\hbar^2} \cdot \frac{1}{(n+\gamma)^2} = -\frac{1}{16}\, \frac{Ry}{(n+\gamma)^2},$$

где Ry (rydberg) $\equiv me^4/(2\hbar^2) = 13.6\,\text{eV}$ is the ionization energy for hydrogen atom in the ground state.

The factor 1/16 reflects the fact that the distance is measured from the surface, what as twice as smaller than the distance between the centers of the probe and image charges.

Flat surface of bulk conducting crystal can be considered as two-dimensional analog of hydrogen atom.

Surface electronic states in the image potential: numerical simulation

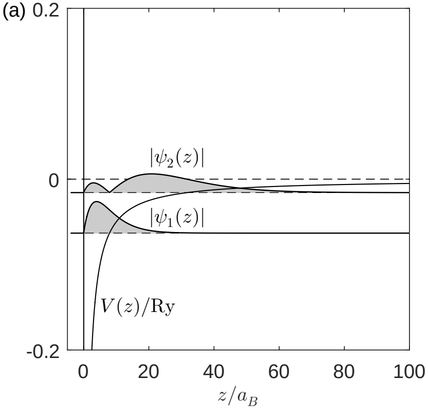

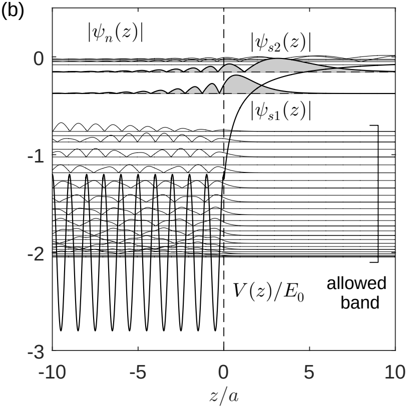

Stark-shifted image-potential states (1)

The shift of the quantum-well states in an uniform electrical field (i. e. in a linearly increasing potential) is analogue of the Stark effect for hydrogen-like atom in electric field.

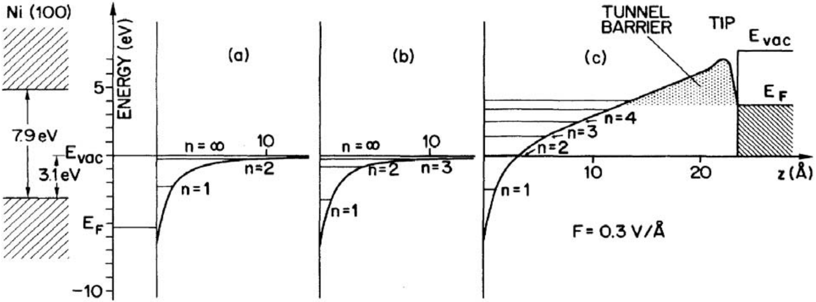

FIG. 1. Energy diagram for the electrostatic potential (including image) at a metal surface. On the left, the projected bulk band structure of the Ni(100) surface is shown shaded. Note the 7.1-eV band gap straddling the vacuum level $E_{vac}=0$. (a) For simplicity, only the $n=1$ and $n=2$ hydrogenic (quantum defect) energy levels are shown. (b) The surface corrugation affects the electronic x,y movement pulling the levels down, as seen by inverse photoemission. (c) Expansion and shift of the image-state spectrum by an applied field, F. The heavy solid line is the crystal potential plus the field potential.

Binnig, Frank, Fuchs, Garcia, Reihl, Rohrer, Salvan,... Phys. Rev. Lett., vol. 55, 991-994 (1985)

Gundlach oscillations of tunneling conductance

Solid-State Electronics Pergamon Press 1966. Vol. 9, pp. 949–957.

$$D \cong \frac{8 \cdot K \cdot \exp\left[-\frac{2}{3} as \frac{W_-^{3/2}}{qV+\Delta\phi}\right]}{2\frac{qV-W_+}{U_0-\Delta\phi}+1+\sin\left[\frac{2}{3} as \frac{(qV-W_+)^{3/2}}{qV+\Delta\phi}\right]}$$

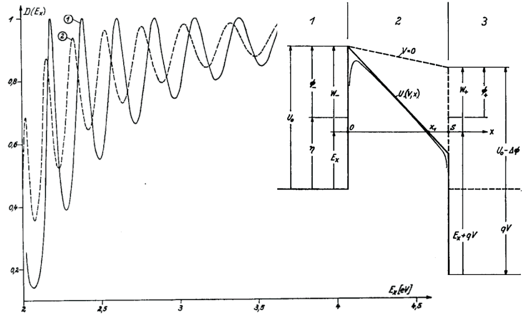

Abb. 4. Durchlässigkeit D als Funktion der kinetischen Energie E_x der einfallenden Elektronen für $E_x \geqslant U_0$, $U_0 = 2$ eV, $a = 1{,}025$ (eV)$^{-1/2}$(Å)$^{-1}$ und $s = 50$ Å.

Kurve 1: $D(E_x)$ nach Gl. (30) für eine rechteckförmige Potentialstufe ($\Delta\phi = V = 0$).

Kurve 2: $D(E_x)$ nach Gl. (18) für eine trapezförmige Potentialstufe ($\Delta\phi = 0{,}5$ eV; $V = 0$).

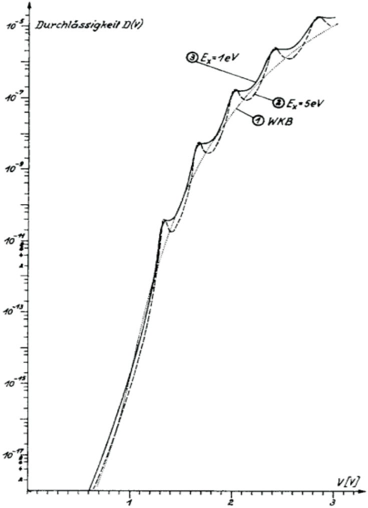

Gundlach, Solid State Electronics, vol. 9, 949-957 (1966)

Stark-shifted image-potential states (2)

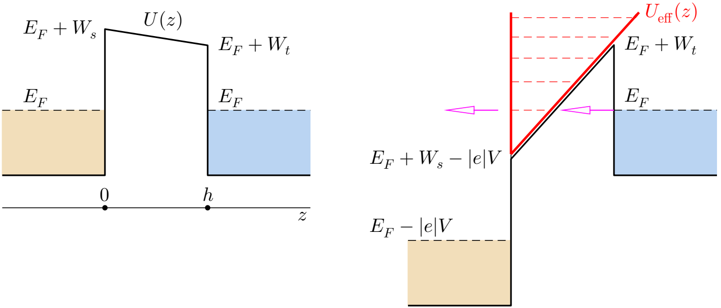

Effective triangular potential well with impenetrable wall at $z = 0$

$$U_{eff}(z) = \begin{cases} \infty & \text{for } z < 0, \\ U^* + F^* \cdot z & \text{for } z \geq 0; \end{cases}$$

where E_F is the chemical potential of electrodes taking into account Volta potential, $U^* = E_F + W_s - |e|V$ is the energy of the bottom of the conduction band, $F^* = (|e|V + W_t - W_s)/h$ is the gradient of the potential energy, proportional to the electric field in the barrier area.

Stark-shifted image-potential states (3)

The Bohr-Sommerfeld quantization rule is

$$\frac{1}{\pi\hbar}\int\limits_a^b p(z)\,dz = n - 1 + \gamma, \qquad n = 1, 2, \dots$$

where $a = 0$ and $b = (E - U^*)/F^*$ are classical turning points, m_0 is mass of electron in vacuum, n is integer index, $\gamma \simeq 3/4$. After substituting $p(z) = \sqrt{2m_0\,(E_n - U_{eff}(z))}$ and integration, we arrive at the spectrum of the quantum-well states

$$E_n = E_F + W_s - |e|U + \left\{\frac{3}{2}\,\frac{\pi\hbar}{\sqrt{2m_0}}\,F_n^*\cdot\left(n - \frac{1}{4}\right)\right\}^{2/3}.$$

Process of resonant tunneling from tip to sample starts provided $E_n \simeq E_F$, then

$$|e|V_n \simeq W_s + \left(\frac{3}{2}\,\frac{\pi\hbar}{\sqrt{2m}}\right)^{2/3}\cdot F_n^{*\,2/3}\cdot\left(n - \frac{1}{4}\right)^{2/3}.$$

An estimate for the energy of the higher-order field-emission resonances ($n \gg 1$)

$$|e|V_n \simeq W_s + \left(\frac{3}{2}\,\frac{\pi\hbar}{\sqrt{2m}}\right)^{2/3}\cdot F_n^{*\,2/3}\cdot n^{2/3}, \quad n = 1, 2, \dots$$

Kolesnychenko, Kolesnichenko, Shklyarevskii, van Kempen, Physica B, v. 291, 246-255 (2000)

Aladyshkin, Journ. Physics: Condens. Matter, v. 32, 435001 (2020)

Typical tunneling spectra: effect of quantum-well states

QWS = quantum-well states, FER = field-emission resonances

amplitude of oscillations of tunneling current at constant mean current and variable height

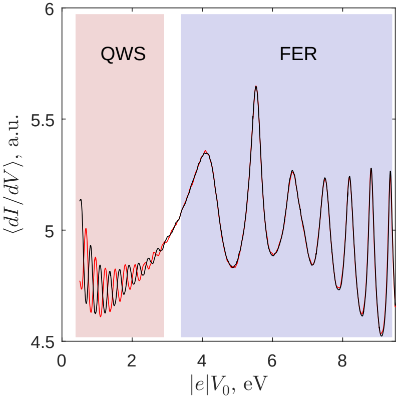

rate of tip displacement at constant mean current and variable height

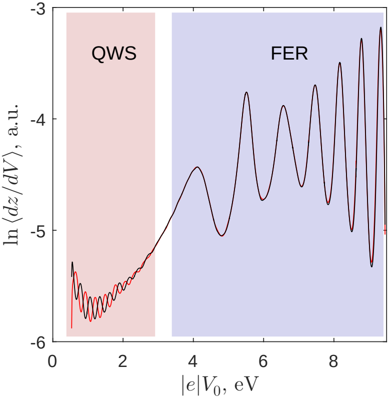

Estimate for local work function for thin Pb(111) films

An estimate for the energy of the higher-order field-emission resonances ($n \gg 1$)

$$|e|V_n \simeq W_s + \left(\frac{3}{2}\frac{\pi\hbar}{\sqrt{2m}}\right)^{2/3} \cdot F_n^{*\,2/3} \cdot n^{2/3}.$$

Tunneling spectra for the same terrace Pb(111), acquired by the STM tip of various shapes of the apex: work function $W_s = 3.8 \pm 0.1$ eV

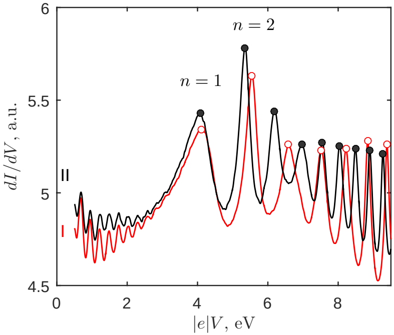

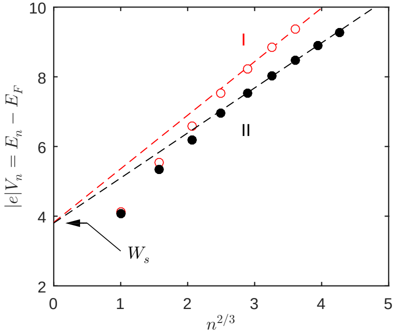

$W_s = 3.85$ eV (theory): Lang and Kohn, Phys. Rev. B 3, 1215 (1971)

Field-emission resonances at $h - U$ diagram: experiment

$$|e|U_n \simeq W_s + \gamma^{2/3} \cdot \left(\frac{|e|U_n + W_t - W_s}{h}\right)^{2/3} \cdot \left(n - \frac{1}{4}\right)^{2/3} \quad \Longrightarrow$$

$$h_n \simeq \alpha \cdot \left(n - \frac{1}{4}\right) \cdot \frac{|e|U + W_t - W_s}{(|e|U - W_s)^{3/2}} \quad \text{and} \quad \delta h = h_{n+1} - h_n \text{ do not depends on } n.$$

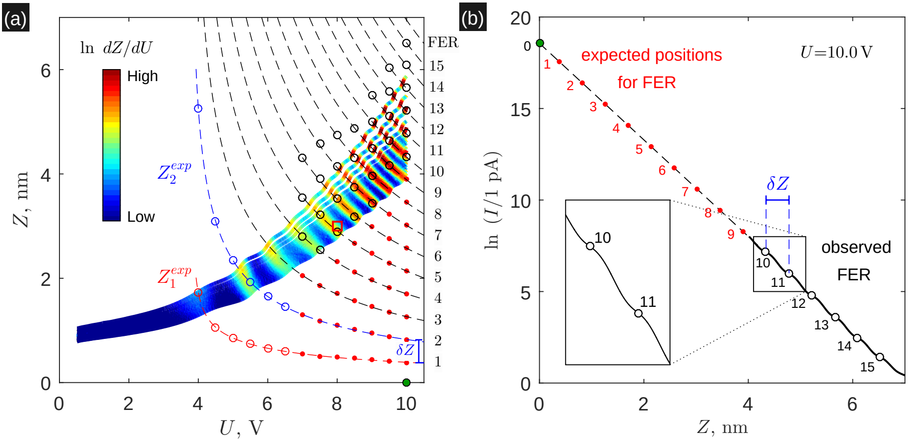

Field-emission resonances and nonexponential dependence of the tunneling current on the STM-tip height

Typical dependence of the tunneling current on the height $I = I_0 \cdot e^{-\alpha \cdot h}$:

$$\alpha = \frac{d(\ln I)}{dh} \simeq -\frac{2\sqrt{2m^*}}{\hbar} \cdot \begin{cases} W^{1/2} & \text{for tunneling regime at } |eU| \ll W; \\ 2W_t^{3/2}/(3|eU|) & \text{for emission regime at } |eU| \gg W. \end{cases}$$

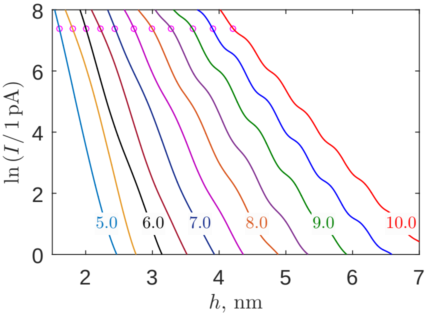

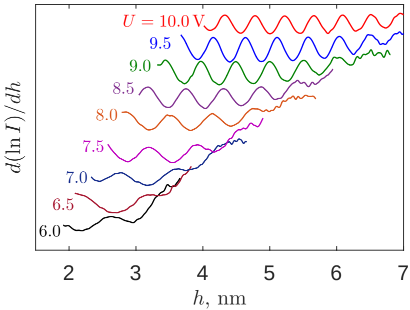

Field-emission resonances are responsible for the bias-dependent periodic variations of the logarithmic derivative $d(\ln I)/dh$ as a function h

Summary (1)

- Electronic properties of thin Pb(111) films grown in single-crystalline Si(111)7×7 and HOPG substrates were studied by low-temperature scanning tunneling microscopy and spectroscopy.

- Analysis of the dependences of differential tunneling conductance dI/dU on bias voltage U for Pb(111) islands of various thickness (from 8 to 50 monolayers) allows us to find experimentally microscopic parameters of Pb(111) films (thickness of wetting layer, Fermi velocity and Fermi wave vector) and determine the $E(k_\perp)$ dependence.

- Peculiar sensitivity of the tunneling spectra $dI/dU(U)$ to the local thickness of the Pb(111) films makes it possible to visualize hidden defects (steps on substrate surface under the metallic layer, inclusions, mechanical stress and nonquantized variations of the height, subsurface dislocation lines).

- We observe periodic oscillations of the visible height of monatomic steps on the Pb(111) surface controlled by quantum-well states in Pb films. The maximum and minimum visible heights of the monatomic Pb(111) step correspond to the bias voltages, at which local densities of states for the Pb(111) terraces of different thicknesses are equal.

Summary (2)

- Using Bohr-Sommerfeld quantization rule for electron in a triangular potential well we derive a simple relationship for the position of the higher field-emission resonances $|e|U_n \simeq W + const \cdot n^{2/3}$, where W is the work function for the sample.
- By analyzing the local spectrum of the field-emission resonances we experimentally determine the local work function for Pb(111) films and demonstrate that this estimate does not depend on tunneling current, shape of the STM tip and the film thickness (for Pb films exceeding 40-50 monolayers).
- We demonstrate that field-emission resonances are responsible for the bias-dependent periodic variations of the logarithmic derivative $d(\ln I)/dh$ as a function h.
- We show that it is possible to find the absolute height of the STM tip above the sample surface without touching the surface.

List of main publications

* Ustavshchikov, Putilov, Aladyshkin, *Tunneling interferometry and measurements of thickness of ultra-thin metallic films Pb(111)* // JETP Lett., vol. 106, 491-497 (2017)

* Putilov, Ustavshchikov, Bozhko, Aladyshkin, *Nonuniform quantum-confined states and visualization of hidden defects in thin Pb(111) films* // JETP Lett., vol. 109, 755-761 (2019)

* Aladyshkin, *Quantum-well and modified image-potential states in thin Pb(111) films: an estimate for the local work function* // Journal of Physics: Condensed Matter, vol. 32, 435001 (2020)

* Aladyshkin, Aladyshkina, Bozhko, *Observation of hidden parts of dislocation loops in thin Pb films by means of scanning tunneling spectroscopy* // Journal of Physical Chemistry C, vol. 125, 26814-26822 (2021)

* Aladyshkin, Schouteden, *Field-emission resonances in thin metallic films: Nonexponential decay of tunneling current as a function of sample-tip distance* // Journal of Physical Chemistry C, vol. 126, 13341–13348 (2022)

* Aladyshkin, *Oscillatory bias dependence of the visible height of the monatomic Pb(111) steps: consequence of the quantum-size effect in thin metallic films* // Journal of Physical Chemistry C, vol. 127, 13295–13301 (2023)

International Symposium 'Nanophysics and Nanoelectronics' Nizhny Novgorod – March 11-15, 2024

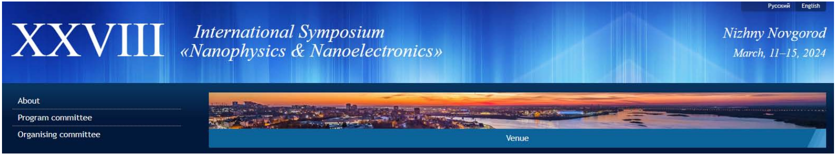

Web-site: **www.nanosymp.ru**   Languages: Russian and English   Participants: > 600

The main sections of the program:

1. Superconducting nanosystems
2. Magnetic nanostructures
3. Semiconductor nanostructures: electronic and optical properties, methods of fabrication
4. Measurements and technologies of atomic and nanometer scale based on probe, electron-beam and ion-beam methods
5. Multilayered and crystalline X-ray optics
6. Element base of quantum solid-state technologies

about 450 km from Moscow to the east

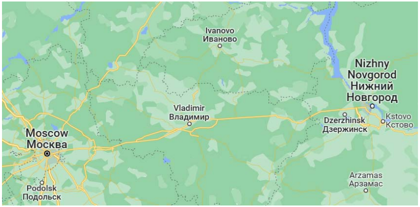

Welcome to Nizhny Novgorod!